Prior and Likelihood Choices for Bayesian Matrix Factorisation on Small Datasets

Thomas Brouwer and **Pietro Lió**
Computer Laboratory, University of Cambridge, United Kingdom

arXiv:1712.00288v1 [stat.ML] 1 Dec 2017

Abstract

In this paper, we study the effects of different prior and likelihood choices for Bayesian matrix factorisation, focusing on small datasets. These choices can greatly influence the predictive performance of the methods. We identify four groups of approaches: Gaussian-likelihood with real-valued priors, nonnegative priors, semi-nonnegative models, and finally Poisson-likelihood approaches. For each group we review several models from the literature, considering sixteen in total, and discuss the relations between different priors and matrix norms. We extensively compare these methods on eight real-world datasets across three application areas, giving both inter- and intra-group comparisons. We measure convergence runtime speed, cross-validation performance, sparse and noisy prediction performance, and model selection robustness. We offer several insights into the trade-offs between prior and likelihood choices for Bayesian matrix factorisation on small datasets—such as that Poisson models give poor predictions, and that nonnegative models are more constrained than real-valued ones.

1 Introduction

Matrix factorisation methods have become very popular in recent years, and used for many applications such as collaborative filtering (Salakhutdinov and Mnih 2008a; Chen, Wang, and Zhang 2009) and bioinformatics (Gönen 2012; Brouwer and Lió 2017). Given a matrix relating two entity types, such as movies and users, matrix factorisation decomposes that matrix into two smaller so-called factor matrices, such that their product approximates the original one. Matrix factorisation is often used for predicting missing values in the datasets, and analysing the resulting factor values to identify biclusters or features.

Most models can be categorised as being either non-probabilistic, such as the popular models by (Lee and Seung 2000), or Bayesian. The former seek to minimise an error function (such as the squared error) between the original matrix and the approximation. In contrast, Bayesian variants treat the two smaller matrices as random variables, place prior distributions over them, and find the posterior distribution over their values after observing the data. A likelihood function, usually Gaussian, is used to capture noise in the dataset. Previous work (Brouwer and Lió 2017) has demonstrated that Bayesian variants are much better for predictive tasks than non-probabilistic versions, which tend to overfit to noise and sparsity.

Matrix factorisation techniques can also be grouped by their constraints on the values in the factor matrices. Firstly, many approaches place no constraints, using real-valued factor matrices (commonly done in the Bayesian literature (Salakhutdinov and Mnih 2008b; Gönen 2012)). Instead, we could constrain them to be nonnegative (as is popular in the non-probabilistic literature (Lee and Seung 2000; Tan and Févotte 2013)), limiting its applicability to nonnegative datasets, but making it easier to interpret the factors and potentially also making the method more robust to overfitting. Thirdly, semi-nonnegative variants constrain one factor matrix to be nonnegative, leaving the other real-valued (Wang, Li, and Zhang 2008; Ding, Li, and Jordan 2010). Finally, some versions work only on count data.

In the Bayesian setting, the first three groups of methods all generally use a Gaussian likelihood for noise, and place either real-valued or nonnegative priors over the matrices. For the former, Gaussian is a common choice (Salakhutdinov and Mnih 2008b; Gönen 2012; Virtanen, Klami, and Kaski 2011; Virtanen et al. 2012), and for the latter options include the exponential distributions (Schmidt, Winther, and Hansen 2009). The fourth group uses a Poisson likelihood to capture count data (Gopalan and Blei 2014; Gopalan, Hofman, and Blei 2015; Hu, Rai, and Carin 2015). These models are often extended by using complicated hierarchical prior structures over the factor matrices, giving additional behaviour (such as automatic model selection).

This paper offers the first systematic comparison between different Bayesian variants of matrix factorisation. Similar comparisons have been provided in other fields, such as for the regression parameter in Bayesian model averaging (Ley and Steel 2009; Eicher, Papageorgiou, and Raftery 2011), which demonstrated that the choice of prior can greatly influence the predictive performance of these models. However, a similar study for Bayesian matrix factorisation is still missing. More strikingly, many papers that introduce new matrix factorisation models do not provide a thorough comparison with competing approaches, or popular non-probabilistic ones such as (Lee and Seung 2000)—for example, the seminal paper by (Salakhutdinov and Mnih 2008b) compares their approach with only one other matrix factorisation method; although (Gopalan, Hofman, and Blei 2015)

compares with three others.

We give an overview of the different approaches that can be found in the literature, including hierarchical priors, and then study the effects of these different Bayesian prior and likelihood choices. We aim to make general statements about the behaviour of the four different groups of methods on small real-world datasets (up to a million observed entries), by considering eight datasets across three different applications—four drug effectiveness datasets, two collaborative filtering datasets, and two methylation expression datasets. Our experiments consider convergence speed, cross-validation performance, sparse and noisy prediction performance, and model selection effectiveness. This study offers novel insights into the differences between the four approaches, and the effects of popular hierarchical priors.

We note that there is a rich literature of Bayesian nonparametric matrix factorisation models, which learn the size of the factor matrices automatically. However, these models often require complex inference approaches to find good solutions, and hence their predictive performance is more determined by the inference method than the precise model choices (such as likelihood and prior). In this paper we therefore focus on parametric matrix factorisation models, to isolate the effects of likelihood and prior choices.

Finally, we acknowledge that the models we study were generally introduced for a specific application domain, and that this makes it hard to make general statements about the behaviour of these methods on different datasets. However, we believe that it is essential to provide a cross-application comparison of the different approaches, as this teaches us valuable lessons for the applications studied, and they are likely to apply to different areas as well. The lack of other studies exploring the trade-offs between likelihood and prior choices for Bayesian matrix factorisation make this a novel and essential study.

2 Bayesian Matrix Factorisation

In this section we introduce the different matrix factorisation models that we study. Formally, the problem of matrix factorisation can be defined as follows. Given an observed matrix $\boldsymbol{R} \in \mathbb{R}^{I \times J}$, we want to find two smaller matrices $\boldsymbol{U} \in \mathbb{R}^{I \times K}$ and $\boldsymbol{V} \in \mathbb{R}^{J \times K}$, each with K so-called factors (columns), to solve $\boldsymbol{R} = \boldsymbol{U}\boldsymbol{V}^T + \boldsymbol{E}$, where noise is captured by matrix $\boldsymbol{E} \in \mathbb{R}^{I \times J}$. Some entries in $\boldsymbol{R}$ may be unobserved, as given by the set $\Omega = \{(i,j) \mid R_{ij} \text{ is observed}\}$. These entries can then be predicted by $\boldsymbol{U}\boldsymbol{V}^T$.

In the Bayesian treatment of matrix factorisation, we express a likelihood function for the observed data that captures noise (such as Gaussian or Poisson). We treat the latent matrices as random variables, placing prior distributions over them. A Bayesian solution for matrix factorisation can then be found by inferring the posterior distribution $p(\boldsymbol{\theta}|D)$ over the latent variables $\boldsymbol{\theta}$ ($\boldsymbol{U}$, $\boldsymbol{V}$, and any additional random variables in our model), given the observed data $D = \{R_{ij}\}_{i,j \in \Omega}$. This posterior distribution is often intractable to compute exactly, but several methods exist to approximate it (see Section 4.1).

In Section 2.2 we introduce a wide range of models from the literature, and categorise them into four groups. The model names are highlighted in bold in the text.

2.1 Probability Distributions

We introduce all notation and probability distributions in the paper below.

$\text{diag}(\boldsymbol{\lambda}^{-1})$ is a diagonal matrix with entries $\lambda_1^{-1}, .., \lambda_K^{-1}$ on the diagonal.

$\mathcal{N}(x|\mu, \tau^{-1}) = \tau^{\frac{1}{2}}(2\pi)^{-\frac{1}{2}} \exp\left\{-\frac{\tau}{2}(x-\mu)^2\right\}$ is a Gaussian distribution with precision τ.

$\mathcal{N}(\boldsymbol{x}|\boldsymbol{\mu}, \boldsymbol{\Sigma}) = |\boldsymbol{\Sigma}|^{-\frac{1}{2}}(2\pi)^{-\frac{K}{2}} \exp\left\{-\frac{1}{2}(\boldsymbol{x}-\boldsymbol{\mu})^T\boldsymbol{\Sigma}^{-1}(\boldsymbol{x}-\boldsymbol{\mu})\right\}$ is a K-dimensional multivariate Gaussian distribution.

$\mathcal{G}(\tau|\alpha_\tau, \beta_\tau) = \frac{{\beta_\tau}^{\alpha_\tau}}{\Gamma(\alpha_\tau)} x^{\alpha_\tau - 1} e^{-\beta_\tau x}$ is a Gamma distribution, where $\Gamma(x) = \int_0^\infty x^{t-1}e^{-x}dt$ is the gamma function.

$\mathcal{NIW}(\boldsymbol{\mu}, \boldsymbol{\Sigma}|\boldsymbol{\mu_0}, \beta_0, \nu_0, \boldsymbol{W_0}) = \mathcal{N}(\boldsymbol{\mu}|\boldsymbol{\mu_0}, \frac{1}{\beta_0}\mathbf{I})\mathcal{W}^{-1}(\boldsymbol{\Sigma}|\nu_0, \boldsymbol{W_0})$ is a normal-inverse Wishart distribution, where $\mathcal{W}^{-1}(\boldsymbol{\Sigma}|\nu_0, \boldsymbol{W_0})$ is an inverse Wishart distribution, and $\mathbf{I}$ the identity matrix.

$\mathcal{L}(x|\mu, \rho) = \frac{1}{2\rho}\exp\left\{-\frac{|x-\mu|}{\rho}\right\}$ is a Laplace distribution.

$\mathcal{IG}(x|\mu, \lambda) = \frac{\lambda}{2\pi x^3}\exp\left\{-\frac{\lambda(x-\mu)^2}{2\mu^2 x}\right\}$ is an inverse Gaussian.

$\mathcal{E}(x|\lambda) = \lambda \exp\{-\lambda x\}\, u(x)$ is an exponential distribution, where $u(x)$ is the unit step function.

$$\mathcal{TN}(x|\mu, \tau) = \begin{cases} \dfrac{\sqrt{\frac{\tau}{2\pi}}\exp\left\{-\frac{\tau}{2}(x-\mu)^2\right\}}{1 - \Phi(-\mu\sqrt{\tau})} & \text{if } x \geq 0 \\ 0 & \text{if } x < 0 \end{cases}$$

is a truncated normal: a normal distribution with zero density below $x = 0$ and renormalised to integrate to one. $\Phi(\cdot)$ is the cumulative distribution function of $\mathcal{N}(0, 1)$.

2.2 Models

There are three types of choices we make that determine the type of matrix factorisation model we use: the likelihood function, the priors we place over the factor matrices $\boldsymbol{U}$ and $\boldsymbol{V}$, and whether we use any further hierarchical priors. We have identified four different groups of Bayesian matrix factorisation approaches based on these choices: Gaussian-likelihood with real-valued priors, nonnegative priors (constraining the matrices $\boldsymbol{U}, \boldsymbol{V}$ to be nonnegative), semi-nonnegative models (constraining one of the two factor matrices to be nonnegative), and finally Poisson-likelihood approaches. Models within each group use different priors and hierarchical priors, and many choices can be found in the literature. In this paper we consider a total of sixteen models, as summarised in Table 1. We have focused on fully conjugate models (meaning the prior and likelihood are in the same family of distributions) to ensure inference for each model is guaranteed to work well, so that all performance differences in Section 6 come entirely from the choice of likelihood and priors.

The first three groups all use a Gaussian likelihood for noise, by assuming each value in $\boldsymbol{R}$ comes from the product of $\boldsymbol{U}$ and $\boldsymbol{V}$, $R_{ij} \sim \mathcal{N}(R_{ij}|\boldsymbol{U_i}\boldsymbol{V_j}, \tau^{-1})$, with Gaussian noise added of precision τ, for which we use a Gamma prior

Table 1: Overview of the Bayesian matrix factorisation models.

Category	Name	Likelihood	Prior $\boldsymbol{U}$	Prior $\boldsymbol{V}$	Hierarchical prior
Real-valued	GGG	$\mathcal{N}(R_{ij}\|\boldsymbol{U_i}\boldsymbol{V_j}, \tau^{-1})$	$\mathcal{N}(\boldsymbol{U_i}\|\boldsymbol{0}, \lambda^{-1}\mathbf{I})$	$\mathcal{N}(\boldsymbol{V_j}\|\boldsymbol{0}, \lambda^{-1}\mathbf{I})$	-
	GGGU	$\mathcal{N}(R_{ij}\|\boldsymbol{U_i}\boldsymbol{V_j}, \tau^{-1})$	$\mathcal{N}(\boldsymbol{U_i}\|\boldsymbol{0}, \lambda^{-1}\mathbf{I})$	$\mathcal{N}(\boldsymbol{V_j}\|\boldsymbol{0}, \lambda^{-1}\mathbf{I})$	-
	GGGA	$\mathcal{N}(R_{ij}\|\boldsymbol{U_i}\boldsymbol{V_j}, \tau^{-1})$	$\mathcal{N}(\boldsymbol{U_i}\|\boldsymbol{0}, \text{diag}(\boldsymbol{\lambda}^{-1}))$	$\mathcal{N}(\boldsymbol{V_j}\|\boldsymbol{0}, \text{diag}(\boldsymbol{\lambda}^{-1}))$	$\lambda_k \sim \mathcal{G}(\alpha_0, \beta_0)$
	GGGW	$\mathcal{N}(R_{ij}\|\boldsymbol{U_i}\boldsymbol{V_j}, \tau^{-1})$	$\mathcal{N}(\boldsymbol{U_i}\|\boldsymbol{\mu_U}, \boldsymbol{\Sigma_U})$	$\mathcal{N}(\boldsymbol{V_j}\|\boldsymbol{\mu_V}, \boldsymbol{\Sigma_V})$	$(\boldsymbol{\mu_U}, \boldsymbol{\Sigma_U})$ and $(\boldsymbol{\mu_V}, \boldsymbol{\Sigma_V})$ $\sim \mathcal{NIW}(\boldsymbol{\mu_0}, \beta_0, \nu_0, \boldsymbol{W_0})$
	GLL	$\mathcal{N}(R_{ij}\|\boldsymbol{U_i}\boldsymbol{V_j}, \tau^{-1})$	$\mathcal{L}(U_{ik}\|0, \eta)$	$\mathcal{L}(V_{jk}\|0, \eta)$	-
	GLLI	$\mathcal{N}(R_{ij}\|\boldsymbol{U_i}\boldsymbol{V_j}, \tau^{-1})$	$\mathcal{L}(U_{ik}\|0, \eta_{ik}^U)$	$\mathcal{L}(V_{jk}\|0, \eta_{jk}^V)$	η_{ik}^U and $\eta_{jk}^V \sim \mathcal{IG}(\mu, \lambda)$
	GVG	$\mathcal{N}(R_{ij}\|\boldsymbol{U_i}\boldsymbol{V_j}, \tau^{-1})$	$p(\boldsymbol{U}) \propto$ $\exp\{-\gamma \det(\boldsymbol{U}^T\boldsymbol{U})\}$	$\mathcal{N}(\boldsymbol{V_j}\|\boldsymbol{0}, \lambda^{-1}\mathbf{I})$	-
Nonnegative	GEE	$\mathcal{N}(R_{ij}\|\boldsymbol{U_i}\boldsymbol{V_j}, \tau^{-1})$	$\mathcal{E}(U_{ik}\|\lambda)$	$\mathcal{E}(V_{jk}\|\lambda)$	-
	GEEA	$\mathcal{N}(R_{ij}\|\boldsymbol{U_i}\boldsymbol{V_j}, \tau^{-1})$	$\mathcal{E}(U_{ik}\|\lambda_k)$	$\mathcal{E}(V_{jk}\|\lambda_k)$	$\lambda_k \sim \mathcal{G}(\alpha_0, \beta_0)$
	GTT	$\mathcal{N}(R_{ij}\|\boldsymbol{U_i}\boldsymbol{V_j}, \tau^{-1})$	$\mathcal{TN}(U_{ik}\|\mu_U, \tau_U)$	$\mathcal{TN}(V_{jk}\|\mu_V, \tau_V)$	-
	GTTN	$\mathcal{N}(R_{ij}\|\boldsymbol{U_i}\boldsymbol{V_j}, \tau^{-1})$	$\mathcal{TN}(U_{ik}\|\mu_U, \tau_U)$	$\mathcal{TN}(V_{jk}\|\mu_V, \tau_V)$	$p(\mu_{ik}^U, \tau_{ik}^U\|\mu_\mu, \tau_\mu, a, b) \propto$ $\frac{1}{\sqrt{\tau_{ik}^U}}\left(1 - \Phi(-\mu_{ik}^U\sqrt{\tau_{ik}^U})\right)$ $\mathcal{N}(\mu_{ik}^U\|\mu_\mu, \tau_\mu^{-1})\mathcal{G}(\tau_{ik}^U\|a, b)$
	GL_1^2	$\mathcal{N}(R_{ij}\|\boldsymbol{U_i}\boldsymbol{V_j}, \tau^{-1})$	$p(\boldsymbol{U}) \propto \exp$ $\{-\frac{\lambda}{2}\sum_i(\sum_k U_{ik})^2\}$ with $U_{ik} \geq 0$	$p(\boldsymbol{V}) \propto \exp$ $\{-\frac{\lambda}{2}\sum_j(\sum_k V_{jk})^2\}$ with $V_{jk} \geq 0$	-
Semi-nonnegative	GEG	$\mathcal{N}(R_{ij}\|\boldsymbol{U_i}\boldsymbol{V_j}, \tau^{-1})$	$\mathcal{E}(U_{ik}\|\lambda)$	$\mathcal{N}(\boldsymbol{V_j}\|\boldsymbol{0}, \lambda^{-1}\mathbf{I})$	-
	GVnG	$\mathcal{N}(R_{ij}\|\boldsymbol{U_i}\boldsymbol{V_j}, \tau^{-1})$	GVG with $U_{ik} \geq 0$	$\mathcal{N}(\boldsymbol{V_j}\|\boldsymbol{0}, \lambda^{-1}\mathbf{I})$	-
Poisson	PGG	$\mathcal{P}(R_{ij}\|\boldsymbol{U_i}\boldsymbol{V_j})$	$\mathcal{G}(U_{ik}\|a, b)$	$\mathcal{G}(V_{jk}\|a, b)$	-
	PGGG	$\mathcal{P}(R_{ij}\|\boldsymbol{U_i}\boldsymbol{V_j})$	$\mathcal{G}(U_{ik}\|a, h_i^U)$	$\mathcal{G}(V_{jk}\|a, h_j^V)$	h_i^U and $h_j^V \sim \mathcal{G}(a', \frac{a'}{b'})$

$\mathcal{G}(\tau|\alpha_\tau, \beta_\tau)$. The last group instead opt for a Poisson likelihood, $R_{ij} \sim \mathcal{P}(R_{ij}|\boldsymbol{U_i}\boldsymbol{V_j})$. This only works for nonnegative count data, with $\boldsymbol{R} \in \mathbb{N}^{I\times J}$, but has been studied extensively in the literature due to the popularity and prevalence of datasets like the Netflix Challenge.

Real-valued matrix factorisation The most common approach is to use independent zero-mean Gaussian priors for $\boldsymbol{U}, \boldsymbol{V}$ (Salakhutdinov and Mnih 2008b; Gönen 2012; Virtanen, Klami, and Kaski 2011; Virtanen et al. 2012), which gives rise to the **GGG** model. The **GGGU** model is identical but uses a univariate posterior for inference (see supplementary materials).

The first hierarchical model (**GGGA**) uses the Bayesian automatic relevance determination (ARD) prior, which helps with model selection. The main idea is to replace the λ hyperparameter by a factor-specific variable λ_k, which has a further Gamma prior. This causes all entries in columns of $\boldsymbol{U}$ and $\boldsymbol{V}$ to go further to zero if only a few values in that column are high, effectively making the factor inactive. This prior has been used for real-valued (Virtanen, Klami, and Kaski 2011; Virtanen et al. 2012) and nonnegative matrix factorisation (Tan and Févotte 2013).

Another hierarchical model (**GGGW**) was introduced in the seminal paper of (Salakhutdinov and Mnih 2008b). Instead of assuming independence of each entry in $\boldsymbol{U}, \boldsymbol{V}$, we assume each row of $\boldsymbol{U}$ comes from a multivariate Gaussian with row mean $\boldsymbol{\mu_U}$ and covariance $\boldsymbol{\Sigma_U}$, and similarly for $\boldsymbol{V}$. We then place a further Normal-Inverse Wishart prior over these parameters.

An alternative to the Gaussian prior is to use the Laplace distribution (Jing, Wang, and Yang 2015), which has a much more pointy distribution than Gaussian around $x = 0$. This leads to more sparse solutions, as more factors are set to low values. The basic model (**GLL**) can be extended with a hierarchical Inverse Gaussian prior over the η parameter (**GLLI**), which they claim helps with variable selection.

The final model (**GVG**) was introduced by (Arngren, Schmidt, and Larsen 2011). They used a volume prior for the $\boldsymbol{U}$ matrix, with density $p(\boldsymbol{U}) \propto \exp\{-\gamma \det(\boldsymbol{U}^T\boldsymbol{U})\}$. The γ hyperparameter determines the strength of the volume penalty (higher means stronger prior).

Nonnegative matrix factorisation These models all place nonnegative prior distributions over entries in $\boldsymbol{U}$ and $\boldsymbol{V}$, and as a result can only deal with nonnegative datasets.

(Schmidt, Winther, and Hansen 2009) introduced a model using exponential priors over the factor matrices (**GEE**). This model can also be extended with ARD (Brouwer, Frellsen, and Lió 2017) (**GEEA**). Another option is to use the truncated normal distribution (**GTT**), which can also be extended by placing a hierarchical prior over the mean and precision $\mu_U, \tau_U, \mu_V, \tau_V$ (**GTTN**), as done by (Schmidt and Mohamed 2009). This nontrivial prior cannot be sampled

from directly, but will be useful for inference.

Finally, we can use a prior inspired by the L_1^2 norm for both $\boldsymbol{U}$ and $\boldsymbol{V}$ ($\mathbf{GL_1^2}$), as we will discuss in Section 3.

Semi-nonnegative matrix factorisation Instead of forcing nonnegativity on both factor matrices, we could place this constraint on only one, as was done in (Wang, Li, and Zhang 2008; Ding, Li, and Jordan 2010). In the Bayesian setting we place a real-valued prior over one matrix, and a nonnegative prior over the other. The major advantage is that we can handle real-valued datasets, while still enforcing some nonnegativity. However, we will see in Section 6 that its performance is identical to the real-valued approaches.

Firstly we can use an exponential prior for entries in $\boldsymbol{U}$, and a Gaussian for $\boldsymbol{V}$, effectively combining the GGG and GEE models into one (**GEG**). Another semi-nonnegative model (**GVnG**) comes from constraining the volume prior in the GVG model to also be nonnegative: $p(\boldsymbol{U}) = 0$ if any $U_{ik} < 0$.

Poisson likelihood The standard Poisson matrix factorisation model (**PGG**) uses independent Gamma priors over the entries in $\boldsymbol{U}$ and $\boldsymbol{V}$, with hyperparameters a, b (Gopalan and Blei 2014; Gopalan, Hofman, and Blei 2015; Hu, Rai, and Carin 2015). This model can also be extended with a hierarchical prior (**PGGG**), by replacing b with h_i^U, h_j^V and placing a further Gamma prior over these parameters (Gopalan, Hofman, and Blei 2015).

3 Priors and Norms

The prior distributions in Bayesian models act as a regulariser that prevents us from overfitting to the data, preventing poor predictive performance. We can write out the expression of the log posterior of the parameters, which for a Gaussian likelihood and no hierarchical priors becomes

$$\begin{aligned}\log p(\boldsymbol{\theta}|D) &= \log p(D|\boldsymbol{\theta}) + \log p(\boldsymbol{\theta}) + C_1 \\ &= \sum_{(i,j)\in\Omega} \log p(R_{ij}|\boldsymbol{U_i V_j}, \tau^{-1}) + \log p(\boldsymbol{U}, \boldsymbol{V}) + C_2 \\ &= -\frac{\tau}{2} \sum_{(i,j)\in\Omega} (R_{ij} - \boldsymbol{U_i V_j})^2 + \log p(\boldsymbol{U}, \boldsymbol{V}) + C_3\end{aligned}$$

for some constants C_i. Note that this last expression is simply the negative Frobenius norm (squared error) of the training fit, plus a regularisation term over the matrices $\boldsymbol{U}, \boldsymbol{V}$. This training error is frequently used in the nonprobabilistic matrix factorisation literature (Lee and Seung 2000; Pauca et al. 2004; Pauca, Piper, and Plemmons 2006), where different regularisation terms are used. These are often based on row-wise **matrix norms**, such as

$$\mathrm{L}_1 = \sum_{i=1}^{I}\sum_{k=1}^{K} U_{ik} \qquad \mathrm{L}_2 = \sum_{i=1}^{I}\sqrt{\sum_{k=1}^{K} U_{ik}}$$

$$\mathrm{L}_1^2 = \sum_{i=1}^{I}(\sum_{k=1}^{K} U_{ik})^2 \qquad \mathrm{L}_2^2 = \sum_{i=1}^{I}\sum_{k=1}^{K} U_{ik}^2$$

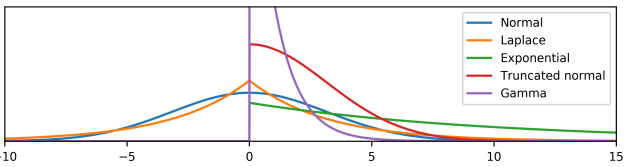


Figure 1: Plots of the prior distributions with hyperparameters from Section 4.2.

This offers some interesting insights: the L_2^2 norm is equivalent to an independent Gaussian prior (GGG), due to the square in the exponential of the Gaussian prior; the L_1 norm is equivalent to a Laplace prior distribution (GLL); if we constrain $\boldsymbol{U}, \boldsymbol{V}$ to be nonnegative then the L_1 norm is equivalent to an exponential prior distribution (GEE); and finally, the L_1^2 norm can be formulated as a nonnegative prior distribution, which we use for the GL_1^2 model (see Table 1).

In other words, the type of priors chosen for Bayesian matrix factorisation determine the type of regularisation that we add to the model. Additionally, we can use hierarchical priors to model further desired behaviour (such as ARD).

4 Model Discussion

4.1 Inference

In this paper we use Gibbs sampling (see Section 4.1), because it tends to be very accurate at finding the true posterior (Brouwer, Frellsen, and Lió 2017), but other methods like variational Bayesian inference are also possible. The Gibbs sampling algorithms, together with their time complexities, are given in the supplementary materials.

4.2 Hyperparameters

The hyperparameter values we choose for each model can influence their performance, especially when the data is sparse. The hierarchical models try to automatically choose the correct values, by placing a prior over the original hyperparameters. This introduces new hyperparameters, but the models are generally less sensitive to these.

However, in our experience even the models without hierarchical priors are not very sensitive to this choice, as long as we use fairly weak priors. In particular, we used $\lambda = 0.1$ (GGG, GGGU, GEE, GTT, GL_1^2, GEG), $\eta = \sqrt{10}$ (GLL), and $a = 1, b = 1$ (PGG). The distributions with these hyperparameter values are plotted in Figure 1.

For the other models we used: $\alpha_\tau = \beta_\tau = 1$ (Gaussian likelihood); $\alpha_0 = \beta_0 = 1$ (GGGA, GEEA); $\boldsymbol{\mu_0} = \mathbf{0}, \beta_0 = 1, \nu_0 = K, \boldsymbol{W_0} = \mathbf{I}$ (GGGW); $\mu = \lambda = K$ (GLLI), $\mu_\mu = 0, \tau_\mu = 0.1, a = b = 1$ (GTTN), $a = a' = b' = 1$ (PGGG).

We did find that the volume prior models (GVG, GVnG) were very sensitive to the hyperparameter choice γ. The following values were chosen by trying a range on each dataset and choosing the best one: $\gamma = 10^{\{-30,-20,-10,-10,0,0,0,0\}}$ for {GDSC,CTRP,CCLE IC_{50},EC_{50},MovieLens 100K,1M,GM,PM}.

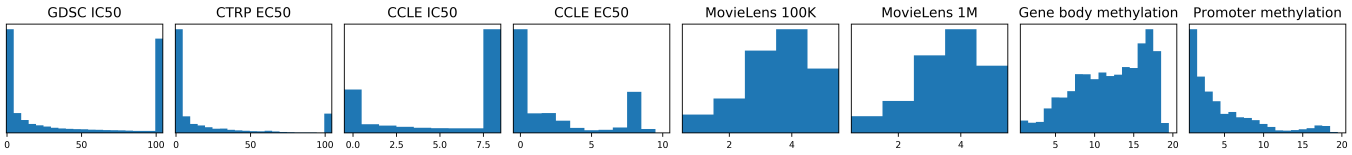


Figure 2: Distributions of the values of the four drug sensitivity, two MovieLens, and two methylation datasets.

Table 2: Overview of the four drug sensitivity, two MovieLens, and two methylation datasets, giving the number of rows (cell lines, users, genes), columns (drugs, movies, patients), and the fraction of entries that are observed.

Dataset	Rows	Columns	Fraction obs.
GDSC IC_{50}	707	139	0.806
CTRP EC_{50}	887	545	0.801
CCLE IC_{50}	504	24	0.965
CCLE EC_{50}	502	24	0.632
MovieLens 100K	943	1473	0.072
MovieLens 1M	6040	3503	0.047
Gene body meth.	160	254	1.000
Promoter meth.	160	254	1.000

4.3 Software

Implementations of all models, datasets, and experiments, are available at `https://github.com/Anonymous/`.

5 Datasets

We conduct our experiments on a total of eight real-world datasets across three different applications, allowing us to see whether our observations on one dataset or application also hold more generally. We will focus on one or two datasets at a time for more specific experiments. Also note that we make sure all datasets contain only positive integers, so that we can compare all four groups of Bayesian matrix factorisation approaches.

The first comes from bioinformatics, in particular predicting missing values in drug sensitivity datasets, each detailing the effectiveness (IC_{50} or EC_{50} values) of a range of drugs on different cancer and tissue types (cell lines). We consider the Genomics of Drug Sensitivity in Cancer (GDSC v5.0 (Yang et al. 2013), IC_{50}), Cancer Therapeutics Response Portal (CTRP v2 (Seashore-Ludlow et al. 2015), EC_{50}), and Cancer Cell Line Encyclopedia (CCLE (Barretina et al. 2012), both IC_{50} and EC_{50}) datasets. We preprocessed these datasets by: undoing the natural log transform of the GDSC dataset; capping high values to 100 for GDSC and CTRP; and then casting them as integers. We also filtered out rows and columns with only one or two observed datapoints.

The second application is collaborative filtering, where we are given movie ratings for different users (one to five stars) and we wish to predict the number of stars a user will give to an unseen movie. We use the MovieLens 100K and 1M datasets (Harper and Konstan 2015), with 100,000 and 1,000,000 ratings respectively.

Finally, another bioinformatics application, this time looking at methylation expression profiles (Koboldt et al. 2012). These datasets give the amount of methylation measured in either the body region of 160 breast cancer driver genes (gene body methylation) or the promoter region (promoter methylation) for 254 different patients. We multiplied all values by twenty and cast them as integers.

The datasets are summarised in Table 2, and the distribution of values for each dataset is visualised in Figure 2. This shows us that the drug sensitivity datasets tend to be bimodal, whereas the MovieLens and methylation datasets are more normally distributed. We can also see that the MovieLens datasets tend to be large and sparse, whereas the others are well-observed and relatively small.

6 Experiments

We conducted experiments to compare the four different groups of approaches. In particular, we measured their convergence speed, cross-validation performance, sparse prediction performance, and model selection effectiveness. We sometimes focus on a selection of the methods for clarity. To make the comparison complete, we also added a popular non-probabilistic nonnegative matrix factorisation model (NMF) (Lee and Seung 2000) as a baseline. The results are discussed in Section 7.

6.1 Convergence

Firstly we compared the convergence speed of the models on the GDSC and MovieLens 100K datasets. We ran each model with $K = 20$, and measured the average mean squared error on the training data across ten runs. We plotted the results in Figure 4, where each group is plotted as the same colour: red for real-valued, blue for nonnegative, green for semi-nonnegative, yellow for Poisson, and grey for the non-probabilistic baseline. Runtime speeds are given in the supplementary materials.

6.2 Cross-validation

Our first predictive experiment was to measure the 5-fold cross-validation performance on each of the eight datasets. We used the hyperparameter values from Section 4.2, and used 5-fold nested cross-validation to choose the dimensionality K. The average mean squared error of predictions are given in Figure 3 for all eight datasets. The average dimensionality found in nested cross-validation can be found in the supplementary materials.

6.3 Noise test

We then measured the predictive performance when the datasets are very noisy. We added different levels of Gaus-

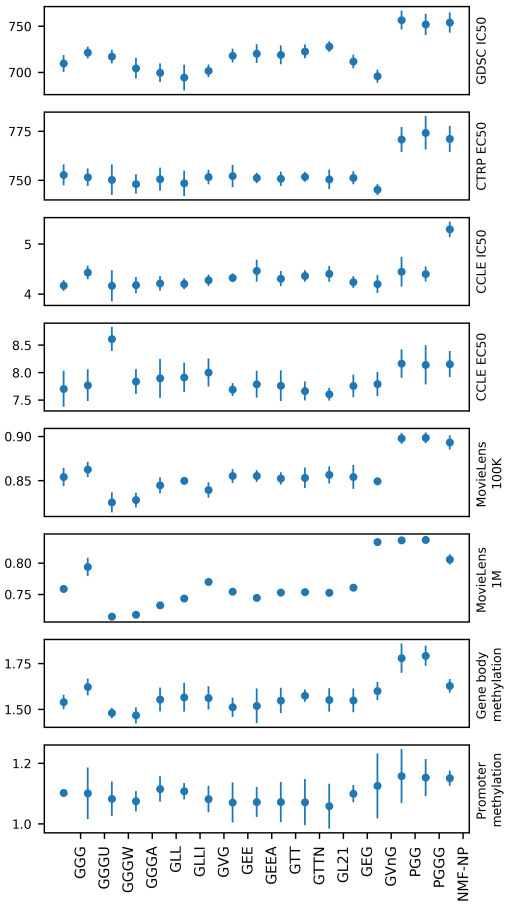


Figure 3: Average mean squared error of 5-fold nested cross-validation for the seventeen methods on the eight datasets. We also plot the standard deviation of errors across the folds.

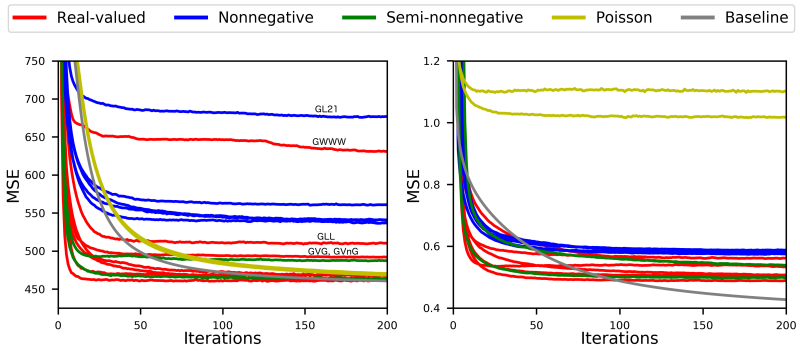


Figure 4: Convergence of the models on the GDSC drug sensitivity (left) and MovieLens 100K (right) datasets, measuring the training data fit (mean square error).

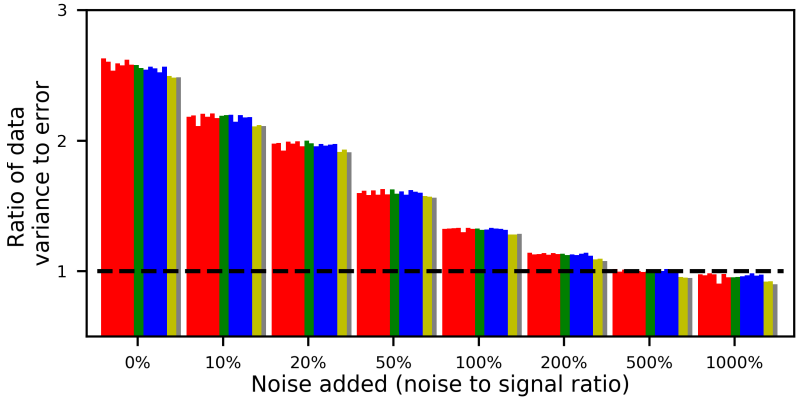


Figure 5: Noise experiment results on the GDSC drug sensitivity dataset. We added different levels of Gaussian noise to the data, and measured the 10-fold cross-validation performance.

sian noise to the data, with the noise-to-signal ratio being given by the ratio of the variance of the Gaussian noise we add, to the standard deviation of the generated data. For each noise level we split the datapoints randomly into ten folds, and measured the predictive performance of the models on one held-out set at a time. We used $K = 5$ for all methods. The results for the GDSC drug sensitivity dataset are given in Figure 5, where we plot the ratio of the variance of the data to the mean squared error of the predictions—higher values are better, and using the row average gives a performance of one.

6.4 Sparse predictions

Next we measured the predictive performances when the sparsity of the data increases. For different fractions of unobserved data, we randomly split the data based on that fraction, trained the model on the observed data, and measured the performance on the held-out test data. We used $K = 5$ for all models. The average mean squared error of ten repeats is given in Figure 6, showing the performances on both the methylation GM and GDSC drug sensitivity datasets.

6.5 Model selection

We also measured the robustness of the models to overfitting if the dimensionality K is high. As a result, most models will fit very well to the training data, but give poor predictions on the test data. Here, we vary the dimensionality K for each of the models on the GDSC drug sensitivity dataset, randomly taking out 10% as test data, and repeating ten times. The results are given in Figure 7—in the supplementary materials we look at two more datasets.

7 Discussion

From the results shown in the previous section, we were able to draw the following conclusions.

Observation 1: Poisson likelihood methods perform poorly compared to the Gaussian likelihood—they overfit quickly (Figures 7a), give worse predictive performances in cross-validation (Figure 3) and under noisy conditions (Figure 5), presumably because they cannot converge as deep as the other methods (Figure 4). At high sparsity levels they can start to perform better (Figure 6d). Some papers (Gopalan, Hofman, and Blei 2015) claim that Poisson models offer bet-

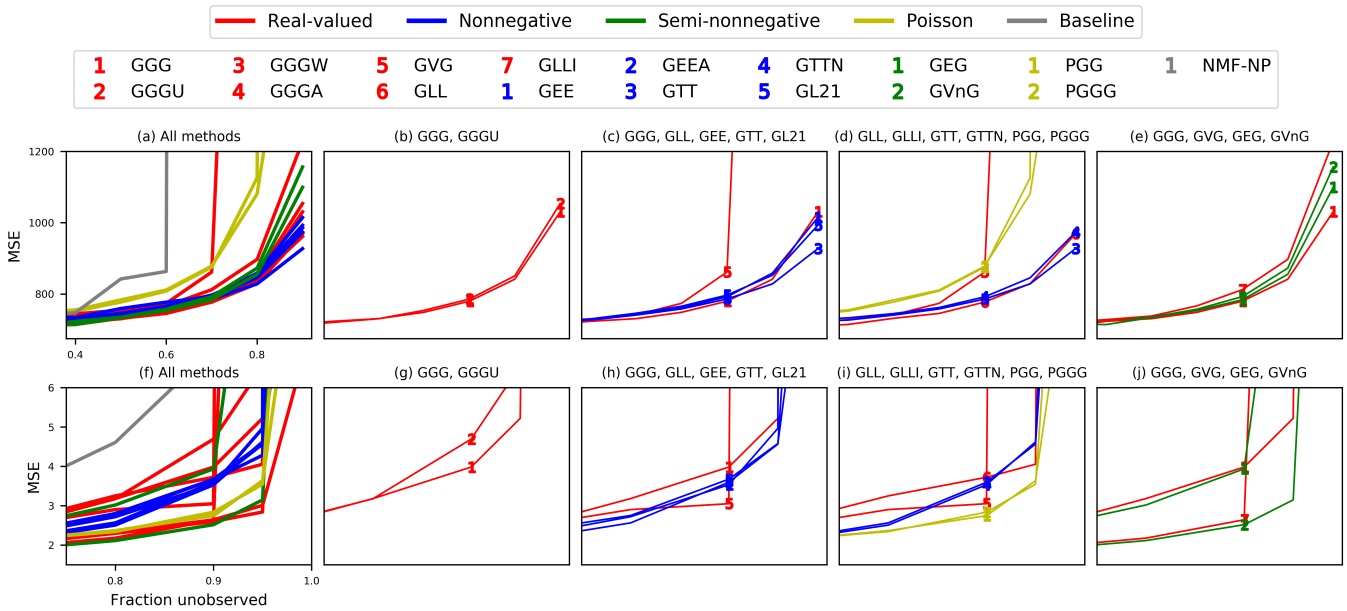


Figure 6: Sparsity experiment results on the GDSC drug sensitivity (top, a-e) and gene body methylation (bottom, f-j) datasets. We measure the predictive performance (mean squared error) on a held-out dataset for different fractions of unobserved data.

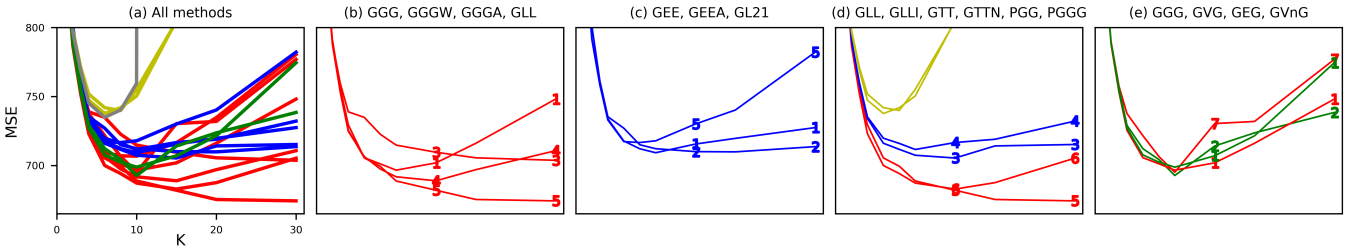


Figure 7: Model selection experiment results on the GDSC drug sensitivity dataset. We measure the predictive performance (mean squared error) on a held-out dataset for different dimensionalities K.

ter predictions, but for small and well-observed datasets we found the opposite to be true.

Observation 2: Nonnegative models are more constrained than the real-valued ones, causing them to converge less deep (Figure 4), and to be less likely to overfit to high sparsity levels (6c, 6h) than the standard GGG model. However, the right hierarchical prior for a real-valued model (such as Wishart) can bridge this gap.

Observation 3: There is no difference in performance between real-valued and semi-nonnegative matrix factorisation, as shown in the model selection and sparsity experiments (Figures 6e, 6j, and 7e): the performance for GGG and GEG, as well as GVG and GVnG, are nearly identical.

Observation 4: There is no difference in predictive performance between univariate and multivariate posteriors (GGG, GGGU), as shown in Figures 6b and 6g.

Observation 5: The automatic relevance determination and Wishart hierarchical priors are effective ways of preventing overfitting, as shown in Figures 7b and 7c: the GGGA, GGGW, and GEEA models keep the line down as K increase, whereas the GGG and GEE models start overfitting more. This has been shown before for nonnegative models (Brouwer, Frellsen, and Lió 2017) but the effect is even stronger for the real-valued ones.

Overvation 6: Similarly, the Laplace priors are good at reducing overfitting as the dimensionality grows (Figure 7b), without requiring additional hierarchical priors.

Observation 7: Some other hierarchical priors do not make a difference, such as with GLLI, GTTN, PGGG—Figures 6d, 6i, and 7d show little difference in performance. They can help us automatically choose the hyperparameters, but in our experience the models are not very sensitive to this choice anyways.

Although these observations are specific to the applications and dataset sizes studied, we believe that general insights can be drawn from them about the behaviour of the four different groups of Bayesian matrix factorisation models. The behaviour of Poisson models is especially interesting, because they are often claimed to be better than Gaussian models for large datasets, but for smaller ones this does not hold. We hope that these insights will assist future researchers in their model design.

References

[Arngren, Schmidt, and Larsen 2011] Arngren, M.; Schmidt, M. N.; and Larsen, J. 2011. Unmixing of Hyperspectral images using bayesian non-negative matrix factorization with volume prior. In *Journal of Signal Processing Systems*, volume 65, 479–496. IEEE.

[Barretina et al. 2012] Barretina, J.; Caponigro, G.; Stransky, N.; Venkatesan, K.; Margolin, A. A.; Kim, S.; Wilson, C. J.; et al. 2012. The Cancer Cell Line Encyclopedia enables predictive modelling of anticancer drug sensitivity. *Nature* 483(7391):603–7.

[Brouwer and Lió 2017] Brouwer, T., and Lió, P. 2017. Bayesian Hybrid Matrix Factorisation for Data Integration. In *Proceedings of the 20th International Conference on Artificial Intelligence and Statistics (AISTATS)*.

[Brouwer, Frellsen, and Lió 2017] Brouwer, T.; Frellsen, J.; and Lió, P. 2017. Comparative Study of Inference Methods for Bayesian Nonnegative Matrix Factorisation. In *Proceedings of the European Conference on Machine Learning and Principles and Practice of Knowledge Discovery in Databases (ECML PKDD)*.

[Chen, Wang, and Zhang 2009] Chen, G.; Wang, F.; and Zhang, C. 2009. Collaborative filtering using orthogonal nonnegative matrix tri-factorization. *Information Processing and Management* 45(3).

[Ding, Li, and Jordan 2010] Ding, C.; Li, T.; and Jordan, M. I. 2010. Convex and semi-nonnegative matrix factorizations. *IEEE Transactions on Pattern Analysis and Machine Intelligence* 32:45–55.

[Eicher, Papageorgiou, and Raftery 2011] Eicher, T. S.; Papageorgiou, C.; and Raftery, A. E. 2011. Default priors and predictive performance in Bayesian model averaging, with application to growth determinants. *Journal of Applied Econometrics* 26(1):30–55.

[Gönen 2012] Gönen, M. 2012. Predicting drug-target interactions from chemical and genomic kernels using Bayesian matrix factorization. *Bioinformatics* 28(18).

[Gopalan and Blei 2014] Gopalan, P., and Blei, D. M. 2014. Bayesian Nonparametric Poisson Factorization for Recommendation Systems. In *Proceedings of the Seventeenth International Conference on Artificial Intelligence and Statistics (AISTATS)*, volume 33, 2–4.

[Gopalan, Hofman, and Blei 2015] Gopalan, P.; Hofman, J. M.; and Blei, D. M. 2015. Scalable recommendation with hierarchical Poisson factorization. In *Proceedings of the Thirty-First Conference on Uncertainty in Artificial Intelligence*, 326–335. AUAI Press.

[Harper and Konstan 2015] Harper, F. M., and Konstan, J. A. 2015. The MovieLens Datasets: History and Context. *ACM Transactions on Interactive Intelligent Systems* 5(4):1–19.

[Hu, Rai, and Carin 2015] Hu, C.; Rai, P.; and Carin, L. 2015. Zero-Truncated Poisson Tensor Factorization for Massive Binary Tensors. In *Uncertainty in Artificial Intelligence (UAI)*.

[Jing, Wang, and Yang 2015] Jing, L.; Wang, P.; and Yang, L. 2015. Sparse Probabilistic Matrix Factorization by Laplace Distribution for Collaborative Filtering. In *Proceedings of the Twenty-Fourth International Joint Conference on Artificial Intelligence (IJCAI)*.

[Koboldt et al. 2012] Koboldt, D. C.; Fulton, R. S.; McLellan, M. D.; Schmidt, H.; Kalicki-Veizer, J.; McMichael, J. F.; Fulton, L. L.; et al. 2012. Comprehensive molecular portraits of human breast tumours. *Nature* 490(7418):61–70.

[Lee and Seung 2000] Lee, D. D., and Seung, H. S. 2000. Algorithms for Non-negative Matrix Factorization. *NIPS, MIT Press* 556–562.

[Ley and Steel 2009] Ley, E., and Steel, M. F. 2009. On the effect of prior assumptions in Bayesian model averaging with applications to growth regression. *Journal of Applied Econometrics* 24(4):651–674.

[Lippert, Weber, and Huang 2008] Lippert, C.; Weber, S.; and Huang, Y. 2008. Relation prediction in multi-relational domains using matrix factorization. In *NIPS workshop on structured input, structured output*.

[Pauca et al. 2004] Pauca, V.; Shahnaz, F.; Berry, M.; and Plemmons, R. 2004. Text mining using non-negative matrix factorizations. In *Proceedings SIAM International Conference on Data Mining (SDM)*, 452–456.

[Pauca, Piper, and Plemmons 2006] Pauca, V. P.; Piper, J.; and Plemmons, R. J. 2006. Nonnegative matrix factorization for spectral data analysis. *Linear Algebra and Its Applications* 416(1):29–47.

[Salakhutdinov and Mnih 2008a] Salakhutdinov, R., and Mnih, A. 2008a. Probabilistic Matrix Factorization. In *Advances in Neural Information Processing Systems (NIPS)*, 1257–1264.

[Salakhutdinov and Mnih 2008b] Salakhutdinov, R., and Mnih, A. 2008b. Bayesian Probabilistic Matrix Factorization using Markov Chain Monte Carlo. In *International Conference on Machine Learning (ICML)*, 880–887. New York, New York, USA: ACM Press.

[Schmidt and Mohamed 2009] Schmidt, M. N., and Mohamed, S. 2009. Probabilistic non-negative tensor factorization using Markov chain Monte Carlo. In *17th European Signal Processing Conference*.

[Schmidt, Winther, and Hansen 2009] Schmidt, M. N.; Winther, O.; and Hansen, L. K. 2009. Bayesian non-negative matrix factorization. In *International Conference on Independent Component Analysis and Signal Separation, Springer Lecture Notes in Computer Science, Vol. 5441*.

[Seashore-Ludlow et al. 2015] Seashore-Ludlow, B.; Rees, M. G.; Cheah, J. H.; Cokol, M.; Price, E. V.; Coletti, M. E.; Jones, V.; et al. 2015. Harnessing Connectivity in a Large-Scale Small-Molecule Sensitivity Dataset. *Cancer discovery* 5(11):1210–23.

[Tan and Févotte 2013] Tan, V. Y. F., and Févotte, C. 2013. Automatic relevance determination in nonnegative matrix factorization with the (β)-divergence. *IEEE Transactions on Pattern Analysis and Machine Intelligence* 35(7):1592–1605.

[Virtanen et al. 2012] Virtanen, S.; Klami, A.; Khan, S.; and Kaski, S. 2012. Bayesian group factor analysis. In *Pro-*

ceedings of the 15th International Conference on Artificial Intelligence and Statistics (AISTATS).

[Virtanen, Klami, and Kaski 2011] Virtanen, S.; Klami, A.; and Kaski, S. 2011. Bayesian CCA via Group Sparsity. In *Proceedings of the 28th International Conference on Machine Learning*.

[Wang, Li, and Zhang 2008] Wang, F.; Li, T.; and Zhang, C. 2008. Semi-supervised clustering via matrix factorization. In *Proceedings of the 2008 SIAM International Conference on Data Mining*.

[Yang et al. 2013] Yang, W.; Soares, J.; Greninger, P.; Edelman, E. J.; Lightfoot, H.; Forbes, S.; Bindal, N.; et al. 2013. Genomics of Drug Sensitivity in Cancer (GDSC): a resource for therapeutic biomarker discovery in cancer cells. *Nucleic acids research* 41(Database issue):D955–61.

arXiv:1712.00288v1 [stat.ML] 1 Dec 2017

Prior and Likelihood Choices for Bayesian Matrix Factorisation on Small Datasets

Supplementary Materials

Thirty-Second AAAI Conference on Artificial Intelligence (2018).

Contents

1 Gibbs sampling algorithms **2**
1.1 Real-valued matrix factorisation 2
1.2 Nonnegative matrix factorisation 5
1.3 Semi-nonnegative matrix factorisation 7
1.4 Poisson matrix factorisation 7

2 Computational complexity **9**

3 Runtime speed **9**

4 Nested cross-validation dimensionalities **10**

5 Sparsity and model selection plots **10**

1 Gibbs sampling algorithms

In this section we give the Gibbs sampling posteriors for the sixteen Bayesian matrix factorisation models studied in the paper.

The idea of Gibbs sampling is as follows. We wish to sample values from the posterior distribution $p(\boldsymbol{\theta}|D)$, but we cannot sample these directly. Instead, we could draw 2values from the conditional posterior $p(\theta_i|\boldsymbol{\theta}_{-i}, D)$, which is the distribution over the parameter θ_i (such as U_{ik}) given the current values of the other parameters $\boldsymbol{\theta}_{-i}$, and the observed data D. If we sample new values in turn for each parameter θ_i from $p(\theta_i|\boldsymbol{\theta}_{-i}, D)$, we will eventually converge to draws from the true posterior $p(\boldsymbol{\theta}|D)$, which can be used to approximate it. In this paper we focus on models where we have so-called *model conjugacy*, allowing us to sample from the conditional posteriors.

We give the Gibbs sampling posterior distributions for $\boldsymbol{U}$, which can be derived using Bayes' theorem. For example, the derivations for U_{ik} in the GEE model can be found below. Expressions for $\boldsymbol{V}$ are symmetrical, and hence omitted.

$$
\begin{aligned}
p(U_{ik}|\tau, \boldsymbol{U}_{-ik}, \boldsymbol{V}, \boldsymbol{\lambda}) &\propto p(\boldsymbol{R}|\tau, \boldsymbol{U}, \boldsymbol{V}) \times p(U_{ik}|\lambda_k) \\
&\propto \prod_{j \in \Omega_i^1} \mathcal{N}(R_{ij}|\boldsymbol{U}_i \cdot \boldsymbol{V}_j, \tau^{-1}) \times \mathcal{E}(U_{ik}|\lambda_k) \\
&\propto \exp\left\{ -\frac{\tau}{2} \sum_{j \in \Omega_i^1} (R_{ij} - \boldsymbol{U}_i \boldsymbol{V}_j)^2 \right\} \times \exp\left\{-\lambda_k U_{ik}\right\} \times u(x) \\
&\propto \exp\left\{ -\frac{U_{ik}^2}{2} \left[\tau \sum_{j \in \Omega_i^1} V_{jk}^2 \right] \right. \\
&\qquad \left. + U_{ik} \left[-\lambda_k + \tau \sum_{j \in \Omega_i^1} (R_{ij} - \sum_{k' \neq k} U_{ik'} V_{jk'}) V_{jk} \right] \right\} \times u(x) \\
&\propto \exp\left\{ -\frac{\tau_{ik}^U}{2} (U_{ik} - \mu_{ik}^U)^2 \right\} \times u(x) \\
&\propto \mathcal{TN}(U_{ik}|\mu_{ik}^U, \tau_{ik}^U).
\end{aligned}
$$

1.1 Real-valued matrix factorisation

The first group of methods use a Gaussian likelihood for noise, and place real-valued prior distributions over $\boldsymbol{U}$ and $\boldsymbol{V}$, typically Gaussian as well. We assume each value in $\boldsymbol{R}$ comes from the product of $\boldsymbol{U}$ and $\boldsymbol{V}$, with Gaussian noise added,

$$
R_{ij} \sim \mathcal{N}(R_{ij}|\boldsymbol{U_i}\boldsymbol{V_j}, \tau^{-1}) \qquad \tau \sim \mathcal{G}(\tau|\alpha_\tau, \beta_\tau)
$$

where $\mathcal{N}(x|\mu, \tau) = \tau^{\frac{1}{2}}(2\pi)^{-\frac{1}{2}} \exp\left\{-\frac{\tau}{2}(x-\mu)^2\right\}$ is the density of the Gaussian distribution, with precision τ. $\boldsymbol{U_i}, \boldsymbol{V_j}$ denote the ith and jth rows of $\boldsymbol{U}$ and $\boldsymbol{V}$. We place a further Gamma prior over τ, with $\mathcal{G}(\tau|\alpha_\tau, \beta_\tau) = \frac{\beta_\tau{}^{\alpha_\tau}}{\Gamma(\alpha_\tau)} x^{\alpha_\tau - 1} e^{-\beta_\tau x}$, where $\Gamma(x) = \int_0^\infty x^{t-1} e^{-x} dt$ is the gamma function.

In the Gibbs sampling algorithm, the posterior for the noise parameter is

$$\tau \sim \mathcal{G}(\tau|\alpha_\tau^*, \beta_\tau^*) \qquad \alpha_\tau^* = \alpha_\tau + \frac{|\Omega|}{2} \qquad \beta_\tau^* = \beta_\tau + \frac{1}{2}\sum_{k=1}^{K}(R_{ij} - \boldsymbol{U_i}\boldsymbol{V_j})^2.$$

1.1.1 All Gaussian model (GGG)

We place Gaussian independent priors over the entries in $\boldsymbol{U}, \boldsymbol{V}$, with hyperparameter λ,

$$\boldsymbol{U_i} \sim \mathcal{N}(\boldsymbol{U_i}|\boldsymbol{0}, \lambda^{-1}\mathbf{I}) \qquad \boldsymbol{V_j} \sim \mathcal{N}(\boldsymbol{V_j}|\boldsymbol{0}, \lambda^{-1}\mathbf{I})$$

where $\mathcal{N}(\boldsymbol{x}|\boldsymbol{\mu}, \boldsymbol{\Sigma}) = |\boldsymbol{\Sigma}|^{-\frac{1}{2}}(2\pi)^{-\frac{K}{2}} \exp\left\{-\frac{1}{2}(\boldsymbol{x}-\boldsymbol{\mu})^T\boldsymbol{\Sigma}^{-1}(\boldsymbol{x}-\boldsymbol{\mu})\right\}$ is the density of a K-dimensional multivariate Gaussian distribution, and $\mathbf{I}$ is the identity matrix. The conditional posterior distributions we obtain in the Gibbs sampling algorithm are also multivariate Gaussians. The parameter values are given below, with $\Omega_i = \{j \mid (i,j) \in \Omega\}$ and $\Omega_j = \{i \mid (i,j) \in \Omega\}$.

$$\boldsymbol{U}_i \sim \mathcal{N}(\boldsymbol{U_i}|\boldsymbol{\mu_i^U}, \boldsymbol{\Sigma_i^U}) \qquad \boldsymbol{\mu_i^U} = \boldsymbol{\Sigma_i^U} \cdot \left[\tau \sum_{j\in\Omega_i} R_{ij}\boldsymbol{V_j}\right] \qquad \boldsymbol{\Sigma_i^U} = \left[\lambda\mathbf{I} + \tau\sum_{j\in\Omega_i}(\boldsymbol{V_j}\otimes\boldsymbol{V_j})\right]^{-1}$$

1.1.2 All Gaussian model with univariate posterior (GGGU)

It is also possible to have a univariate posterior for the Gibbs sampler,

$$U_{ik} \sim \mathcal{N}(U_{ik}|\mu_{ik}^U, (\tau_{ik}^U)^{-1}) \qquad \mu_{ik}^U = \frac{1}{\tau_{ik}^U}\left[\tau\sum_{j\in\Omega_i}(R_{ij} - \sum_{k'\neq k} U_{ik'}V_{jk'})V_{jk}\right] \qquad \tau_{ik}^U = \lambda + \tau\sum_{j\in\Omega_i} V_{jk}^2.$$

1.1.3 All Gaussian model with ARD hierarchical prior (GGGA)

For the automatic relevance determination (ARD) prior we replace the λ hyperparameter by a factor-specific variable λ_k, which has a further Gamma prior.

$$\boldsymbol{U_i} \sim \mathcal{N}(\boldsymbol{U_i}|\boldsymbol{0}, \mathrm{diag}(\boldsymbol{\lambda}^{-1})) \qquad \boldsymbol{V_j} \sim \mathcal{N}(\boldsymbol{V_j}|\boldsymbol{0}, \mathrm{diag}(\boldsymbol{\lambda}^{-1})) \qquad \lambda_k \sim \mathcal{G}(\lambda_k|\alpha_0, \beta_0)$$

where $\mathrm{diag}(\boldsymbol{\lambda}^{-1})$ is a diagonal matrix with entries $\lambda_1^{-1}, .., \lambda_K^{-1}$ on the diagonal. The Gibbs sampling posteriors for $\boldsymbol{U_i}$ and $\boldsymbol{V_j}$ are largely unchanged, replacing $\lambda\mathbf{I}$ in the expressions for $\boldsymbol{\Sigma_i^U}, \boldsymbol{\Sigma_j^V}$ by $\mathrm{diag}(\lambda_1, .., \lambda_K)$. The posterior for λ_k is

$$\lambda_k \sim \mathcal{G}(\lambda_k|\alpha_0^*, \beta_0^*) \qquad \alpha_0^* = \alpha_0 + \frac{I}{2} + \frac{J}{2} \qquad \beta_0^* = \beta_0 + \frac{1}{2}\sum_{i=1}^{I} U_{ik}^2 + \frac{1}{2}\sum_{j=1}^{J} V_{jk}^2.$$

1.1.4 All Gaussian model with Wishart hierarchical prior (GGGW)

Instead of assuming independence of each entry in $\boldsymbol{U}, \boldsymbol{V}$, we now assume each row of $\boldsymbol{U}$ comes from a multivariate Gaussian with row mean $\boldsymbol{\mu_U}$ and covariance $\boldsymbol{\Sigma_U}$, and similarly for $\boldsymbol{V}$. We place a further Normal-Inverse Wishart prior over these parameters,

$$\begin{aligned} \boldsymbol{U_i} &\sim \mathcal{N}(\boldsymbol{U_i}|\boldsymbol{\mu_U}, \boldsymbol{\Sigma_U}) & \boldsymbol{\mu_U}, \boldsymbol{\Sigma_U} &\sim \mathcal{NIW}(\boldsymbol{\mu_U}, \boldsymbol{\Sigma_U}|\boldsymbol{\mu_0}, \beta_0, \nu_0, \boldsymbol{W_0}) \\ \boldsymbol{V_j} &\sim \mathcal{N}(\boldsymbol{V_j}|\boldsymbol{\mu_V}, \boldsymbol{\Sigma_V}) & \boldsymbol{\mu_V}, \boldsymbol{\Sigma_V} &\sim \mathcal{NIW}(\boldsymbol{\mu_V}, \boldsymbol{\Sigma_V}|\boldsymbol{\mu_0}, \beta_0, \nu_0, \boldsymbol{W_0}) \end{aligned}$$

where $\mathcal{NIW}(\boldsymbol{\mu_U}, \boldsymbol{\Sigma_U}|\boldsymbol{\mu_0}, \beta_0, \nu_0, \boldsymbol{W_0}) = \mathcal{N}(\boldsymbol{\mu}|\boldsymbol{\mu_0}, \frac{1}{\beta_0}\mathbf{I})\mathcal{W}^{-1}(\boldsymbol{\Sigma}|\nu_0, \boldsymbol{W_0})$ is the density of a normal-inverse Wishart distribution, and $\mathcal{W}^{-1}(\boldsymbol{\Sigma}|\nu_0, \boldsymbol{W_0})$ is the inverse Wishart distribution.

For the Gibbs sampling algorithm we obtain the posteriors $\boldsymbol{U_i} \sim \mathcal{N}(\boldsymbol{U_i}|\boldsymbol{\mu_i^U}, \boldsymbol{\Sigma_i^U})$ and $\boldsymbol{\mu_U}, \boldsymbol{\Sigma_U} \sim \mathcal{NIW}(\boldsymbol{\mu_U}, \boldsymbol{\Sigma_U}|\boldsymbol{\mu_0^*}, \beta_0^*, \nu_0^*, \boldsymbol{W_0^*})$, with

$$\boldsymbol{\mu_i^U} = \boldsymbol{\Sigma_i^U} \cdot \left[\boldsymbol{\Sigma_U^{-1}}\boldsymbol{\mu_U} + \tau \sum_{j \in \Omega_i} R_{ij}\boldsymbol{V_j}\right] \qquad \boldsymbol{\Sigma_i^U} = \left[\boldsymbol{\Sigma_U^{-1}} + \tau \sum_{j \in \Omega_i} (\boldsymbol{V_j} \otimes \boldsymbol{V_j})\right]^{-1}$$

$$\beta_0^* = \beta_0 + I \qquad \nu_0^* = \nu_0 + I \qquad \boldsymbol{\mu_0^*} = \frac{\beta_0\boldsymbol{\mu_0} + I\bar{\boldsymbol{U}}}{\beta_0 + I} \qquad \bar{\boldsymbol{U}} = \frac{1}{I}\sum_{i=1}^{I} \boldsymbol{U_i}$$

$$\boldsymbol{W_0^*} = \boldsymbol{W_0} + I\bar{\boldsymbol{S}} + \frac{\beta_0 I}{\beta_0 + I}(\boldsymbol{\mu_0} - \bar{\boldsymbol{U}}) \otimes (\boldsymbol{\mu_0} - \bar{\boldsymbol{U}}) \qquad \bar{\boldsymbol{S}} = \frac{1}{I}\sum_{i=1}^{I}(\boldsymbol{U_i} \otimes \boldsymbol{U_i}).$$

1.1.5 Gaussian likelihood with Laplace priors (GLL)

An alternative to the Gaussian prior is to use the Laplace distribution, which has a much more pointy distribution than Gaussian around $x = 0$. This leads to more sparse solutions, as more factors are set to low values. The priors are

$$U_{ik} \sim \mathcal{L}(U_{ik}|0, \eta) \qquad V_{jk} \sim \mathcal{L}(V_{jk}|0, \eta)$$

To simplify inference we introduce a new variable λ_{ik}^U for each U_{ik}, with prior $\lambda_{ik}^U \sim \mathcal{E}(\lambda_{ik}^U|\eta)$. The idea behind this is that we can rewrite a Laplace distribution as

$$\mathcal{L}(x|\mu, \rho) = \int_{\epsilon=0}^{\infty} \mathcal{N}(x|\mu, \epsilon)\mathcal{E}(\epsilon|\frac{\rho}{2})d\epsilon$$

This leads to the following Gibbs sampling posteriors:

$$\boldsymbol{U}_i \sim \mathcal{N}(\boldsymbol{U_i}|\boldsymbol{\mu_i^U}, \boldsymbol{\Sigma_i^U}) \qquad \boldsymbol{\mu_i^U} = \boldsymbol{\Sigma_i^U} \cdot \left[\tau \sum_{j \in \Omega_i} R_{ij}\boldsymbol{V_j}\right]$$

$$\boldsymbol{\Sigma_i^U} = \mathrm{diag}((\boldsymbol{\lambda_i^U})^{-1}) + \left[\tau \sum_{j \in \Omega_i} (\boldsymbol{V_j} \otimes \boldsymbol{V_j})\right]^{-1}$$

$$\frac{1}{\lambda_{ik}^U} \sim \mathcal{IG}(x|\mu_{ik}^U, \lambda_{ik}^U) \qquad \mu_{ik}^U = \frac{\sqrt{\eta}}{|U_{ik}|} \qquad \lambda_{ik}^U = \eta.$$

1.1.6 Gaussian likelihood with Laplace and hierarchical inverse Gaussian priors (GLLI)

We can place a further hierarchical prior over the η parameters,

$$\eta_{ik}^U \sim \mathcal{IG}(\mu, \lambda) \qquad \eta_{jk}^V \sim \mathcal{IG}(\mu, \lambda).$$

The paper that introduced this prior (Jing, Wang and Yang 2015) placed a Generalised Inverse Gaussian $\mathcal{GIG}(\gamma, a, b)$ prior over the η parameters, but then used $\gamma = -\frac{1}{2}$, which reduces the prior to the Inverse Gaussian above with $\mu = \sqrt{b/a}, \lambda = b$ (or $a = 1/\mu, b = \lambda$).

The posteriors for $\boldsymbol{U}, \boldsymbol{V}$ are identical, and for λ_{ik}^U we only replace η with η_{ik}^U. We obtain another Inverse Gaussian posterior for the η_{ik}^U parameters,

$$\eta_{ik}^U \sim \mathcal{IG}(\eta_{ik}^U | \mu_{ik}^\eta, \lambda_{ik}^\eta) \qquad \mu_{ik}^U = \sqrt{\frac{\lambda_{ik}^U + a}{b}} = \sqrt{\frac{\lambda_{ik}^U + 1/\mu}{\lambda}} \qquad \lambda_{ik}^U = \lambda_{ik}^U + b = 1/\mu.$$

1.1.7 Gaussian likelihood with volume prior (GVG)

The prior over $\boldsymbol{V}$ in this model is Gaussian, as in the GGG model, but we now use the volume prior (VP) for the $\boldsymbol{U}$ matrix, with density $p(\boldsymbol{U}) \propto \exp\{-\gamma \det(\boldsymbol{U}^T\boldsymbol{U})\}$. This model leads to the posterior

$$U_{ik} \sim \mathcal{N}(U_{ik} | \mu_{ik}^U, (\tau_{ik}^U)^{-1}) \qquad \mu_{ik}^U = \frac{1}{\tau_{ik}^U}\left[\gamma \boldsymbol{U_{i\tilde{k}}} \boldsymbol{A_{\tilde{k}\tilde{k}}} (\boldsymbol{U_{\tilde{i}\tilde{k}}^T} \boldsymbol{U_{\tilde{i}k}}) + \tau \sum_{j \in \Omega_i} (R_{ij} - \sum_{k' \neq k} U_{ik'} V_{jk'}) V_{jk}\right]$$
$$\tau_{ik}^U = \tau \sum_{j \in \Omega_i} V_{jk}^2 + \gamma (D_{\tilde{k}\tilde{k}} - \boldsymbol{U_{i\tilde{k}}} \boldsymbol{A_{\tilde{k}\tilde{k}}} \boldsymbol{U_{i\tilde{k}}^T}).$$

In the above, vector $\boldsymbol{U_{i\tilde{k}}}$ is the ith row of $\boldsymbol{U}$ excluding column k; vector $\boldsymbol{U_{\tilde{i}k}}$ is the kth column of $\boldsymbol{U}$ excluding row i; matrix $\boldsymbol{U_{\tilde{i}\tilde{k}}}$ is $\boldsymbol{U}$ excluding row i and column k; matrix $\boldsymbol{U_{\cdot\tilde{k}}}$ is $\boldsymbol{U}$ excluding column k; $D_{\tilde{k}\tilde{k}} = \det\{\boldsymbol{U_{\cdot\tilde{k}}^T} \boldsymbol{U_{\cdot\tilde{k}}}\}$; and matrix $\boldsymbol{A_{\tilde{k}\tilde{k}}} = \det\{\boldsymbol{U_{\cdot\tilde{k}}^T} \boldsymbol{U_{\cdot\tilde{k}}}\}$ is the matrix adjugate.

1.2 Nonnegative matrix factorisation

Nonnegative matrix factorisation models use the same Gaussian noise model as the real-valued ones, but placing nonnegative prior distributions over entries in $\boldsymbol{U}$ and $\boldsymbol{V}$.

1.2.1 Gaussian likelihood with exponential priors (GEE)

This model places independent Exponential priors over the entries in $\boldsymbol{U}, \boldsymbol{V}$,

$$U_{ik} \sim \mathcal{E}(U_{ik} | \lambda) \qquad V_{jk} \sim \mathcal{E}(V_{jk} | \lambda).$$

The product of a Gaussian and Exponential distribution leads to a truncated normal posterior,

$$U_{ik} \sim \mathcal{TN}(U_{ik} | \mu_{ik}^U, \tau_{ik}^U) \qquad \mu_{ik}^U = \frac{1}{\tau_{ik}^U}\left[-\lambda + \tau \sum_{j \in \Omega_i} (R_{ij} - \sum_{k' \neq k} U_{ik'} V_{jk'}) V_{jk}\right] \qquad \tau_{ik}^U = \tau \sum_{j \in \Omega_i} V_{jk}^2.$$

1.2.2 Gaussian likelihood with exponential prior and ARD (GEEA)

Similar to the GGGA model, we can extend GEE with the ARD prior,

$$U_{ik} \sim \mathcal{E}(U_{ik} | \lambda_k) \qquad V_{jk} \sim \mathcal{E}(V_{jk} | \lambda_k) \qquad \lambda_k \sim \mathcal{G}(\lambda_k | \alpha_0, \beta_0)$$

The posteriors for $\boldsymbol{U}$ and $\boldsymbol{V}$ are the same as in the GEE model, but replacing λ by λ_k. The posteriors for λ_k become

$$\lambda_k \sim \mathcal{G}(\lambda_k | \alpha_0^*, \beta_0^*) \qquad \alpha_0^* = \alpha_0 + I + J \qquad \beta_0^* = \beta_0 + \sum_{i=1}^{I} U_{ik} + \sum_{j=1}^{J} V_{jk}.$$

1.2.3 Gaussian likelihood with truncated normal priors (GTT)

We can also use the truncated normal distribution directly as the priors for $\boldsymbol{U}$ and $\boldsymbol{V}$,

$$U_{ik} \sim \mathcal{TN}(U_{ik}|\mu_U, \tau_U) \qquad V_{jk} \sim \mathcal{TN}(V_{jk}|\mu_V, \tau_V)$$

This again gives a truncated normal posterior, but with slightly different values.

$$U_{ik} \sim \mathcal{TN}(U_{ik}|\mu^U_{ik}, (\tau^U_{ik})^{-1}) \qquad \mu^U_{ik} = \frac{1}{\tau^U_{ik}}\left[\mu_U\tau_U + \tau\sum_{j\in\Omega_i}(R_{ij} - \sum_{k'\neq k} U_{ik'}V_{jk'})V_{jk}\right]$$
$$\tau^U_{ik} = \tau_U + \tau\sum_{j\in\Omega_i} V^2_{jk}.$$

An alternative to the truncated normal distribution is the so-called half normal. If random variable y has density $\mathcal{N}(y|0,\sigma^2)$, and random variable $x = |y|$, then x follows a half normal distribution with density $\mathcal{HN}(x|\sigma) = \frac{\sqrt{2}}{\sigma\sqrt{\pi}}\exp\{-\frac{x^2}{2\sigma^2}\}u(x)$. Note however that when $\mu = 0$ in the truncated normal distribution, then these distributions are equivalent, with $\tau = \frac{1}{\sigma^2}$, so the GTT model is more general.

1.2.4 Gaussian likelihood with truncated normal and hierarchical priors (GTTN)

We can place a further prior over the parameters of the truncated normal distributions,

$$U_{ik} \sim \mathcal{TN}(U_{ik}|\mu^U_{ik}, \tau^U_{ik}) \qquad V_{jk} \sim \mathcal{TN}(V_{jk}|\mu^V_{jk}, \tau^V_{jk})$$
$$p(\mu^U_{ik}, \tau^U_{ik}|\mu_\mu, \tau\mu, a, b) \propto \frac{1}{\sqrt{\tau^U_{ik}}}\left(1 - \Phi(-\mu^U_{ik}\sqrt{\tau^U_{ik}})\right)\mathcal{N}(\mu^U_{ik}|\mu_\mu, \tau_\mu^{-1}).\mathcal{G}(\tau^U_{ik}|a,b)$$

The density for μ^V_{jk}, τ^V_{jk} is identical. Note that this is not the same as the product of a Normal and Gamma distribution. It is not easy to sample from this prior, but it can be used as a hierarchical prior. The posteriors for U_{ik} remain the same (replacing μ_U and τ_U by μ^U_{ik} and τ^U_{ik}), and for μ^U_{ik} and τ^U_{ik} we obtain posteriors

$$\mu^U_{ik} \sim \mathcal{N}(\mu^U_{ik}|m_\mu, t_\mu^{-1}) \qquad m_\mu = \frac{1}{t_\mu}\left[\tau^U_{ik}U_{ik} + \mu_\mu\tau_\mu\right] \qquad t_\mu = \tau^U_{ik} + \tau_\mu$$
$$\tau^U_{ik} \sim \mathcal{G}(\tau^U_{ik}|a^*, b^*) \qquad a^* = a + \frac{1}{2} \qquad b^* = b + \frac{(U_{ik} - \mu^U_{ik})^2}{2}.$$

1.2.5 Gaussian likelihood with $\mathbf{L_1^2}$ norm priors ($\mathbf{GL_1^2}$)

We can also use a prior inspired by the L_1^2 norm for both $\boldsymbol{U}$ and $\boldsymbol{V}$, giving prior densities

$$p(\boldsymbol{U}) \propto \begin{cases} \exp\{-\frac{\lambda}{2}\sum_i\left(\sum_k U_{ik}\right)^2\} & \text{if } U_{ik} \geq 0 \text{ for all } i,k \\ 0 & \text{if any } U_{ik} < 0 \end{cases}$$
$$p(\boldsymbol{V}) \propto \begin{cases} \exp\{-\frac{\lambda}{2}\sum_j\left(\sum_k V_{jk}\right)^2 & \text{if } V_{jk} \geq 0 \text{ for all } j,k \\ 0 & \text{if any } V_{jk} < 0 \end{cases}$$

The nonnegativity constraint is used to address the fact that the L_1^2 norm used the absolute value of entries in $\boldsymbol{U}, \boldsymbol{V}$, which makes inference impossible unless we constrain them to be nonnegative (in which case the values are automatically absolute).

The posteriors are similar to the GEE and GTT models, but now adding a term that depends on the other entries in the ith (or jth) row of $\boldsymbol{U}$,

$$U_{ik} \sim \mathcal{TN}(U_{ik}|\mu_{ik}^U, \tau_{ik}^U) \qquad \mu_{ik}^U = \frac{1}{\tau_{ik}^U}\left[-\lambda \sum_{k' \neq k} U_{ik'} + \tau \sum_{j \in \Omega_i} (R_{ij} - \sum_{k' \neq k} U_{ik'} V_{jk'}) V_{jk} \right]$$
$$\tau_{ik}^U = \lambda + \tau \sum_{j \in \Omega_i} V_{jk}^2.$$

1.3 Semi-nonnegative matrix factorisation

In the nonnegative matrix factorisation models we placed nonnegative priors over both $\boldsymbol{U}$ and $\boldsymbol{V}$. Instead, we could constrain only one to be nonnegative. In the Bayesian setting this is done by placing a real-valued prior over one matrix, and a nonnegative prior over the other. The major advantage is that we can handle real-valued datasets, while still enforcing some nonnegativity.

1.3.1 Gaussian likelihood with nonnegative volume prior (GVnG)

The volume prior discussed earlier can also be formulated to be nonnegative. In particular, the probability distribution over $\boldsymbol{U}$ is

$$p(\boldsymbol{U}) \propto \begin{cases} \exp\{-\gamma \det(\boldsymbol{U}^T \boldsymbol{U})\} & \text{if } U_{ik} \geq 0 \text{ for all } i,k \\ 0 & \text{if any } U_{ik} < 0 \end{cases}$$

The posterior parameters are the same as for the GVG model, but drawing new values from a truncated normal, rather than normal. For $\boldsymbol{V}$ we again use a Gaussian.

1.3.2 Gaussian likelihood with exponential and Gaussian priors (GEG)

For this model we use an exponential prior for entries in $\boldsymbol{U}$, and a Gaussian for $\boldsymbol{V}$. The posteriors are given in the GEE and GGG model sections.

1.4 Poisson matrix factorisation

The final category of matrix factorisation models do not use a Gaussian likelihood, instead opting for a Poisson one. This only works for nonnegative count data, with $\boldsymbol{R} \in \mathbb{N}^{I \times J}$. We again assume each value in $\boldsymbol{R}$ comes from the product of $\boldsymbol{U}$ and $\boldsymbol{V}$, $R_{ij} \sim \mathcal{P}(R_{ij}|\boldsymbol{U_i V_j})$, where $\mathcal{P}(x|\lambda) = \frac{\lambda^x \exp\{-\lambda\}}{x!}$ is the density of a Poisson distribution.

1.4.1 Poisson likelihood with Gamma priors (PGG)

The standard Poisson matrix factorisation model uses independent Gamma priors over the entries in $\boldsymbol{U}$ and $\boldsymbol{V}$. To make inference simpler, we also introduce random variables Z_{ijk}

such that $R_{ij} = \sum_{k=1}^{K} Z_{ijk}$, each effectively accounting for the contribution of factor k to R_{ij}. We use the following distributions and priors:

$$Z_{ijk} \sim \mathcal{P}(Z_{ijk}|U_{ik}V_{jk}) \qquad U_{ik} \sim \mathcal{G}(U_{ik}|a,b) \qquad V_{jk} \sim \mathcal{G}(V_{jk}|a,b).$$

Note that we can do this because the sum of Poisson distributed random variables (like Z_{ijk}) is again Poisson distributed, with rate λ equal to the sum of rates of the Z_{ijk}, giving us the original Poisson likelihood for R_{ij}. The above is also equivalent to saying that $\boldsymbol{Z_{ij}} \sim \text{Mult}(\boldsymbol{Z_{ij}}|n,\boldsymbol{p})$ with $n = R_{ij}$ and $\boldsymbol{p} = (\frac{U_{i1}V_{j1}}{\boldsymbol{U_iV_j}}, .., \frac{U_{iK}V_{jK}}{\boldsymbol{U_iV_j}})$, where $\boldsymbol{Z_{ij}}$ is a vector containing $Z_{ij1}, .., Z_{ijK}$, and $\text{Mult}(\boldsymbol{x}|n,\boldsymbol{p}) = \frac{n!}{x_1!..x_K!}p_1^{x_1}..p_K^{x_K}$ is a K-dimensional multinomial distribution.

Using the above trick, the posteriors are

$$\begin{aligned}
&\boldsymbol{Z_{ij}} \sim \text{Mult}(\boldsymbol{Z_{ij}}|n,\boldsymbol{p}) \qquad n = R_{ij} \qquad \boldsymbol{p} = (\frac{U_{i1}V_{j1}}{\boldsymbol{U_iV_j}}, .., \frac{U_{iK}V_{jK}}{\boldsymbol{U_iV_j}}) \\
&U_{ik} \sim \mathcal{P}(U_{ik}|a^*_{ik}, b^*_{ik}) \qquad a^*_{ik} = a + \sum_{j\in\Omega_i} Z_{ijk} \qquad b^*_{ik} = b + \sum_{j\in\Omega_i} V_{jk}.
\end{aligned}$$

1.4.2 Poisson likelihood with Gamma and hierarchical Gamma priors (PGGG)

We can extend the standard Poisson matrix factorisation model with hierarchical priors. The priors are

$$U_{ik} \sim \mathcal{G}(U_{ik}|a, h^U_i) \qquad V_{jk} \sim \mathcal{G}(V_{jk}|a, h^V_j) \qquad h^U_i \sim \mathcal{G}(a', \frac{a'}{b'}) \qquad h^V_j \sim \mathcal{G}(a', \frac{a'}{b'})$$

The posteriors for U_{ik} are identical to the PGG model, except replacing b with h^U_i in the expression for b^*_{ik}. For the hierarchical part we obtain the following posteriors:

$$h^U_i \sim \mathcal{G}(h^U_i|a^*_i, b^*_i) \qquad a^*_i = a' + Ka \qquad b^*_i = \frac{a'}{b'} + \sum_{k=1}^{K} U_{ik}.$$

2 Computational complexity

The different matrix factorisation models have different time complexities for computing the parameter values and sample new values for $\boldsymbol{U}$, $\boldsymbol{V}$, and any other random variables. The space complexity for all models is $\mathcal{O}(IK + JK)$ per iteration, with an additional $K|\Omega|$ term for the Poisson models (for the Z_{ijk}).

The time complexities per iteration for the multivariate Gaussian posterior models (GGG, GGGA, GGGW, GLL, GLLI) is $\mathcal{O}((I + J)K^3 + IJK^2)$. However, these row draws and parameter value computations can all be done in parallel. The univariate posterior models (GGGU, GEE, GEEA, GTT, GTTN, GL_1^2, GEG) have complexity $\mathcal{O}(IJK^2)$, but the parameters can be computed efficiently per column. The volume prior models (GVG, GVnG) have the highest complexity, with $\mathcal{O}(I^2JK^2)$. Finally, the Poisson models are $\mathcal{O}(IJK)$, but this hides a big constant that effectively makes it the slowest model for low values of K.

3 Runtime speed

The average runtime (in seconds) per iteration is given in Table 1, for different values of K on the GDSC drug sensitivity and MovieLens 100K datasets. Here we see that the univariate posterior models (GGGU, GEE, GEEA, GTT, GTTN, GL_1^2, GEG) are faster than the multivariate ones (GGG, GGGA, GGGW, GLL, GLLI); models with hierarchical priors are not noticably slower; the volume prior models are by far the slowest, due to their higher time complexity; and the Poisson models are slow for low K, but at higher values this is no longer true.

Table 1: Average runtime per iteration (in seconds) on GDSC drug sensitivity and MovieLens 100K.

	GDSC drug sensitivity				MovieLens 100K			
Method	$K = 5$	$K = 10$	$K = 20$	$K = 50$	$K = 5$	$K = 10$	$K = 20$	$K = 50$
GGG	0.14	0.18	0.29	0.93	1.04	1.29	1.86	5.07
GGGU	0.02	0.03	0.07	0.16	0.48	0.79	1.49	3.99
GGGA	0.14	0.17	0.28	0.93	1.03	1.30	1.88	5.75
GGGW	0.13	0.17	0.26	0.82	1.27	1.23	1.84	5.06
GLL	0.24	0.30	0.38	0.95	0.81	0.94	1.30	3.01
GLLI	0.22	0.29	0.42	0.98	0.82	0.99	1.49	3.26
GVG	0.42	1.02	2.58	22.1	1.22	2.86	5.94	40.9
GEE	0.06	0.12	0.25	0.66	0.49	0.86	1.68	4.16
GEEA	0.06	0.12	0.24	0.63	0.68	1.27	2.53	6.50
GTT	0.06	0.12	0.25	0.68	0.70	1.27	2.34	6.00
GTTN	0.07	0.14	0.29	0.77	0.71	1.22	2.55	6.56
GL_1^2	0.06	0.13	0.26	0.62	0.43	0.80	1.56	3.88
GVnG	0.45	1.16	2.88	22.9	2.02	5.08	9.63	53.2
GEG	0.07	0.12	0.22	0.61	0.96	1.30	1.34	3.51
PGG	0.36	0.40	0.50	0.78	1.32	1.96	3.36	7.07
PGGG	0.56	0.49	0.50	0.78	1.34	2.02	3.40	7.19
NMF-NP	0.01	0.04	0.04	0.16	0.32	0.52	1.11	2.62

4 Nested cross-validation dimensionalities

In the main paper we used nested cross-validation to find the best dimensionality K in each fold of the cross-validation. Table 2 contains the average values for each model on each dataset, rounded to the nearest integer. We used these values for the noise and sparsity experiments, to give each model their own optimal starting point. The models with ARD and Wishart priors (GGGA, GGGW, GEEA) and with the volume prior (GVG, GVnG) can often leverage higher dimensionalities K than the others.

For reference, the cross-validation performances are provided in Figure 1.

Table 2: Average dimensionality found in 5-fold nested cross-validation for each method on the eight datasets.

	Drug sensitivity				MovieLens		Methylation	
Method	GDSC	CTRP	CCLE IC_{50}	CCLE EC_{50}	100K	1M	Gene body	Promoter
GGG	6	4	5	1	2	5	4	3
GGGU	6	5	5	1	2	2	3	3
GGGA	10	6	5	1	4	10	6	3
GGGW	16	8	6	2	5	13	7	3
GLL	10	6	5	1	3	8	4	2
GLLI	10	6	5	1	2	7	4	2
GVG	10	5	6	2	3	3	4	4
GEE	8	6	5	1	2	8	6	5
GEEA	10	6	5	1	2	10	6	4
GTT	9	6	5	1	2	8	5	4
GTTN	8	6	5	1	2	8	5	4
GL_1^2	6	6	4	1	2	8	5	5
GEG	6	5	5	1	2	5	4	3
GVnG	11	8	5	2	2	1	3	3
PGG	4	2	13	1	1	1	2	3
PGGG	5	2	12	1	1	1	2	3
NMF	4	2	1	1	1	3	2	2

5 Sparsity and model selection plots

Although we presented results for the sparsity and model selection experiments on only a few datasets, we ran them both on the GDSC drug sensitivity, MovieLens 100K, and gene body methylation datasets. We give the results in Figures 2 and 3.

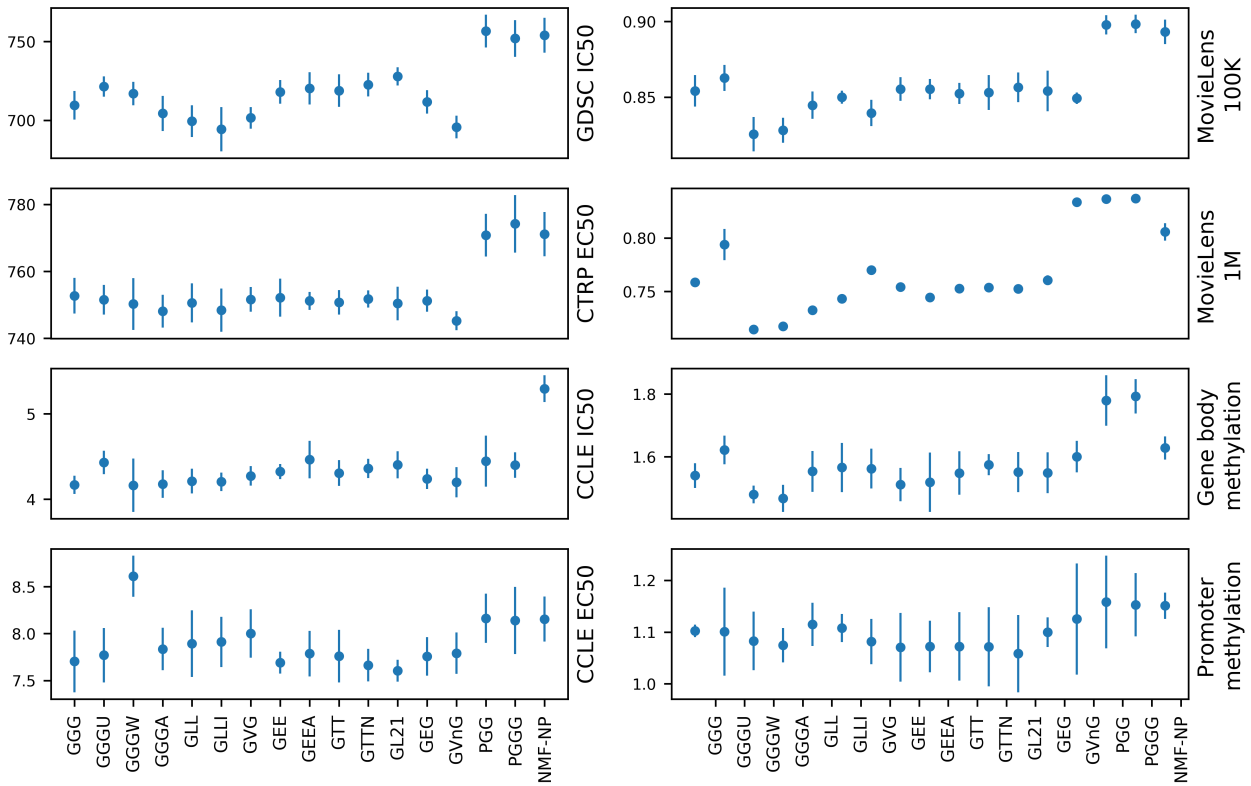


Figure 1: Average mean squared error of 5-fold nested cross-validation for the seventeen methods on the eight datasets. We also plot the standard deviation of errors across the folds.

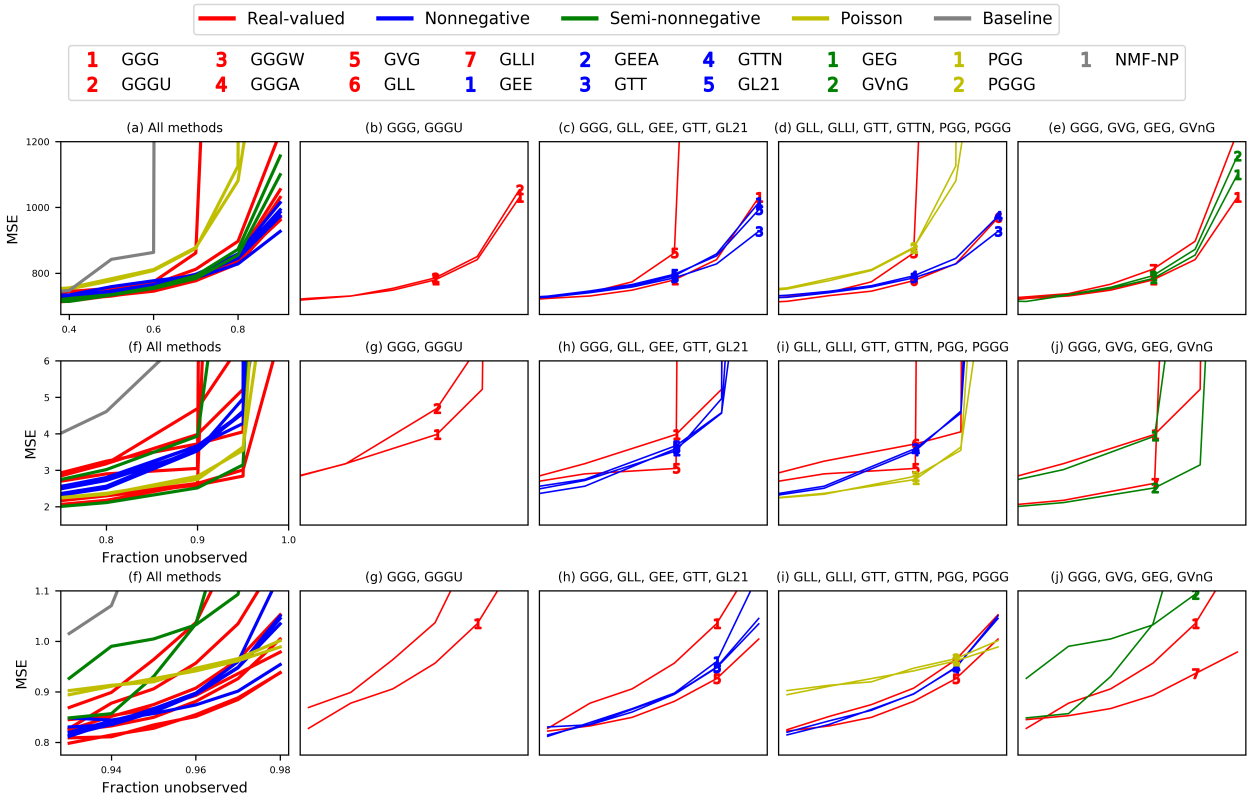


Figure 2: Sparsity experiment results on the GDSC drug sensitivity (top, a-e), gene body methylation (middle, f-j), and MovieLens 100K (bottom, k-o) datasets. We measure the predictive performance (mean squared error) on a held-out dataset for different fractions of unobserved data.

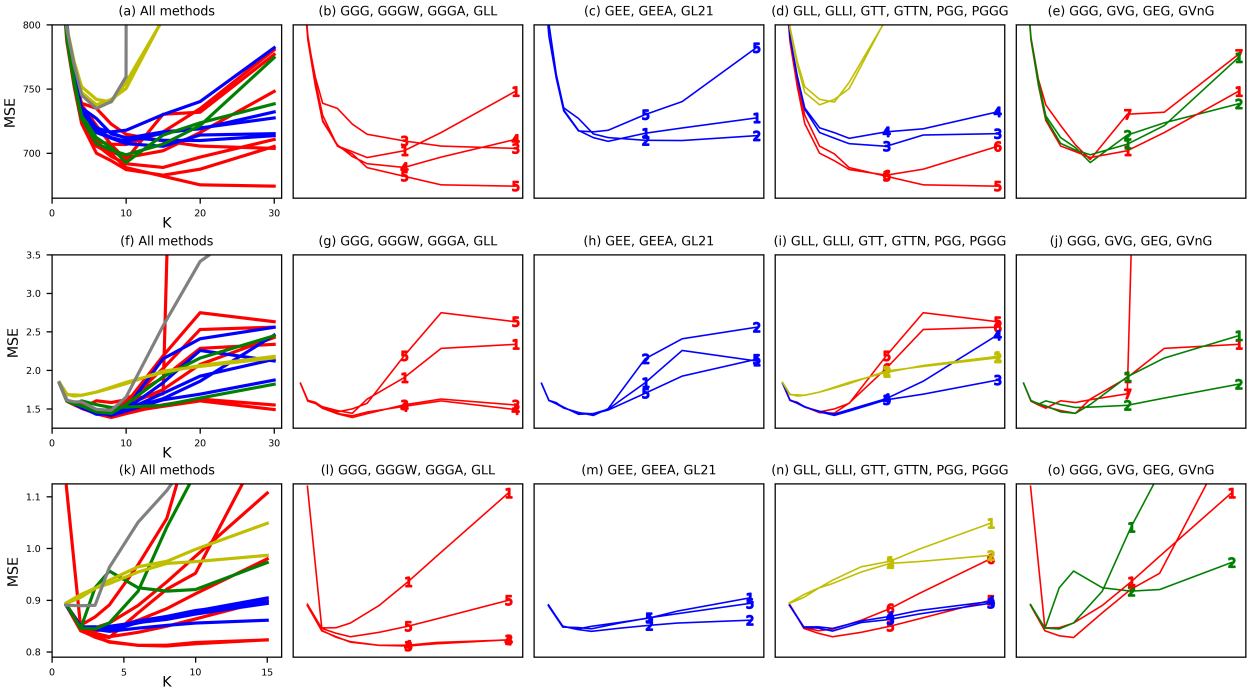


Figure 3: Model selection experiment results on the GDSC drug sensitivity (top, a-e), gene body methylation (middle, f-j), and MovieLens 100K (bottom, k-o) datasets. We measure the predictive performance (mean squared error) on a held-out dataset for different dimensionalities K.